Bloch waves and band structure for diffracted and channeled particles in crystals

Gershon Kurizki*
Institute for Modern Optics, Department of Physics and Astronomy, University of New Mexico, Albuquerque, New Mexico 87131
(Received 2 July 1984; revised manuscript received 9 May 1985)

Comprehensive, detailed studies of radiative and inelastic-scattering transitions of fast charged particles propagating in crystals require improvements in the description of their Bloch eigenfunctions and quasimomentum bands. Progress towards achieving the required description is made here by (a) introducing a general iterative treatment of the effects of the crystal-potential variation along the direction of the particle propagation on the Bloch eigenfunctions, and (b) employing Hill's-equation theory to analyze, in a unified fashion, the various diffraction regimes (including the planar channeling regime) for particles which enter the crystal at small angles relative to a set of low-index crystal planes [the systematic-reflection geometry (SRG)]. Among the results obtained for diffraction in the SRG the most notable are the following: (1) analytical expressions for the band structure and the Bloch eigenfunctions for electrons and positrons (β particles) with energies $\lesssim 1$ MeV; (2) expressions revealing the existence of gaps between bands populated by β particles with energies up to a few hundred MeV (or nonrelativistic mesons) whose propagation transverse to the set of crystal planes is unbounded; (3) analytical estimates of tunneling into the vicinity of atomic sites and of the bandwidth, for states occupied by positrons in the planar channeling regime.

I. INTRODUCTION

The diffraction of a fast charged particle (i.e., a particle whose kinetic energy E_K is anywhere above a few tens of a keV) in a crystal[1-5] at small angles relative to a low-index crystal axis or plane is described fairly well in the projection approximation.[6-8] In this approximation the propagation of the particle in the direction(s) parallel to the axis (plane), hereafter referred to as the longitudinal direction(s), is assumed to be free. This assumption is equivalent to the replacement of the crystal potential by its average over the longitudinal coordinate(s), known as the projected potential, which is periodic in the transverse coordinate(s). The transverse propagation is then investigated by (a) determining the eigenvalue bands [transverse energy bands (TEB's)] (Refs. 9–11) and Bloch eigenfunctions (waves) of the Schrödinger equation for a particle whose mass is $(1 + E_K/mc^2)m$, m being its rest mass in the projected potential, and (b) finding the population amplitudes of these Bloch eigenstates for a given direction of incidence of the particle. As the relativistic mass of the particle increases, this description gradually approaches the classical picture of quasifree or channeling trajectories, depending on the populated TEB's.[12-14] Although the projection approximation is commonly used, effects of the longitudinal variation of the potential (LVP hereafter) on diffraction have also been noted.[15,16]

It is argued below that the prevailing analytical models[6,7,10,12,16] do not yield certain features of the diffraction that affect the radiation emitted by diffracted particles[17-19] or their inelastic scattering.[20-23] The present treatment is aimed at improving the tools for analytical studies of these processes,[24] particularly with regard to the following physical properties.

A. Longitudinal-mode (LM) radiation intensity

The existence of LM radiation, which results from the effects of the LVP on the particle, has been recently demonstrated in the pioneering experiments of Spence *et al.*,[25,26] following its theoretical prediction.[27-29] The peak frequencies of LM radiation have been calculated[25-30] to the accuracy required for the above experiments. In contrast, the spectral distribution of its intensity is still not well understood. Even its numerical evaluation, based on three-dimensional many-beam equations, has encountered difficulties, being highly time-consuming.[26] The present treatment of LVP effects is intended to allow a facile, yet highly accurate, analysis of LM radiation intensity.

B. The spectrum of unbound transverse energies

The prevailing assumption until recently has been that, for relativistic particles, unbound transverse energies (above the projected-potential maxima) form practically a continuum.[12,31-33] This assumption has been unable to explain the spectrum of radiation resulting from transitions between unbound transverse energy states.[34] In a recent work[35] a formalism has been developed which allows computation of the unbound TEB structure for the special case of a periodic Pöschl-Teller potential. A far more general analysis of the unbound TEB's, valid for any one-dimensional centrosymmetric periodic potential, is given here. It demonstrates the existence of sizeable gaps between unbound bands for relativistic particles. These gaps must be taken into account in the analysis of the emitted radiation, according to the scheme outlined in Ref. 30.

C. Bandwidths and tunneling strength in the channeling regime

Semiqualitative estimates of bandwidths in the channeling regime have been given analytically for electrons only,[36] whereas for channeled positrons only numerical calculations of bandwidths have been performed.[37-39] These calculations have shown that bandwidth effects are

significant for the radiation emitted by positrons occupying highly excited, transversely bound states. As will be shown here, this implies that tunneling into classically forbidden regions in the vicinity of atomic sites is nonnegligible for such positrons and should contribute to their inelastic scattering. The present treatment considerably facilitates the evaluation of bandwidths and tunneling strengths for channeled particles.

In addition to pursuing the above specific objectives, in this paper we seek to unify the treatment of the variety of diffraction regimes determined by the relativistic mass of the particle and its direction of incidence. Such unification is required for a complete analysis of the radiation emitted by the particle[24] or of its inelastic scattering, since these processes can cause transitions between different regimes.

This article is organized as follows. In Sec. II an iterative procedure is constructed, which produces the Fourier components of the Bloch eigenfunction that are generated by the longitudinal potential variation. Those Fourier components which arise due to diffraction in the projected potential serve as input. Unlike previous attempts, this procedure is carried out here to the accuracy required for LM radiation calculations. The subsequent discussion is restricted to diffraction in a one-dimensional centrosymmetric projected potential, characterizing particles incident at small angles relative to a single set of low-index crystal planes. This geometrical situation allows extensive investigation of the Bloch eigenfunctions and transverse energy eigenvalues, using the powerful Hill's-equation method, which has not been applied hitherto to diffraction problems. In Sec. III it is shown that the asymptotic forms of the eigenfunctions and eigenvalues strongly depend on a dimensionless parameter, thereafter referred to as potential depth. In Sec. IV the "shallow"-potential situation is analyzed, the analysis covering both kinematic and dynamic diffraction of electrons and positrons with energies up to a few MeV. In Sec. V we deal with the "deep"-potential situation, which pertains to transversely unbound as well as channeled particles whose relativistic mass is much larger than the electron rest mass. In Sec. VI we summarize the results of this treatment.

Additional details and topics are found in Chap. 2 of Ref. 29, on which this article is mostly based. These include discussions of effects of noncentrosymmetric projected potentials and of the "intermediate-depth"-potential situation.

II. LONGITUDINAL AND TRANSVERSE DIFFRACTION

A. Premises of the treatment

The aim of the following treatment is to take account of LVP effects in a manner which is more suitable for LM-emission calculations than that of previously suggested methods. We start with a brief exposition of known results which will be the premises for the ensuing treatment. The negligibility of spin-orbit (spin-lattice) coupling for a spin-$\frac{1}{2}$ fast particle in a crystal[40,41] implies that the spatial amplitude of its energy eigenfunctions satisfies the Klein-Gordon equation. We assume that the particle is incident on the crystal as a plane wave $\exp(i\mathbf{k}_0\cdot\mathbf{r})$. Upon ignoring crystal-surface effects,[42,43] the Klein-Gordon equation can then be cast, to first order in V/E (the ratio of the potential energy of the particle in the crystal to its total energy), into the following set of equations, using the Bloch form of the eigenfunctions $\psi_E(\mathbf{r})$:[6,7]

$$[k_0^2-U_0-(\mathbf{k}+\mathbf{g})^2]c_{\mathbf{g}}^{(\mathbf{k})}-\sum_{\mathbf{g}'(\neq 0)}U_{\mathbf{g}'}c_{\mathbf{g}-\mathbf{g}'}^{(\mathbf{k})}=0\ . \tag{1}$$

Here we have used the Fourier decomposition

$$\psi_E^{(\mathbf{k})}(\mathbf{r})=\sum_{\mathbf{g}}c_{\mathbf{g}}^{(\mathbf{k})}e^{i(\mathbf{k}+\mathbf{g})\cdot\mathbf{r}}\ , \tag{2a}$$

$$U(\mathbf{r})=\frac{2E}{\hbar^2c^2}V(\mathbf{r})\equiv\frac{2m\gamma}{\hbar^2}V(\mathbf{r})=\sum_{\mathbf{g}}U_{\mathbf{g}}e^{i\mathbf{g}\cdot\mathbf{r}}\ , \tag{2b}$$

the $\mathbf{g}$'s being all reciprocal-lattice vectors (RLV's) with any allowed three-dimensional components. The "beam coefficients" (BC's) $c_{\mathbf{g}}^{(\mathbf{k})}$ are normalized by

$$\sum_{\mathbf{g}}|c_{\mathbf{g}}^{(\mathbf{k})}|^2=1\ . \tag{2c}$$

The $\psi_E^{(\mathbf{k})}(\mathbf{r})$ and $c_{\mathbf{g}}^{(\mathbf{k})}$ are labeled by the quasimomentum $\hbar\mathbf{k}$, which is required by the continuity condition at the surface, taken to be normal to $\mathbf{z}$, to satisfy

$$\mathbf{k}=k_{0x}\hat{\mathbf{x}}+k_{0y}\hat{\mathbf{y}}+k_z\hat{\mathbf{z}}\ . \tag{3}$$

The potential used in Eq. (2b) contains the Debye-Waller factor.

The $c_{\mathbf{g}}^{(\mathbf{k})}$ and $\mathbf{k}$ satisfying Eqs. (2) (which describe the diffraction of the particle due to its elastic scattering by the crystal potential) constitute the input required for calculations of (1) the radiative-transition matrix elements and emission frequencies,[18,19,24–30] (2) the effects of inelastic scattering on the diffraction pattern,[20–22] and (3) the radiation linewidths.[23]

Two generic geometries are commonly considered in treatments of fast particles diffracted in crystals. Assuming the surfaces $z=\pm L/2$ of the crystal slab to be perpendicular to a RLV set $g_z\hat{\mathbf{z}}$ and parallel to a RLV set $g_x\hat{\mathbf{x}}+g_y\hat{\mathbf{y}}$, these geometries are[6,12] the following: (1) $\mathbf{r}_\perp\equiv(x,y)$,

$$k_{0\parallel}\equiv k_{0z}\gg|\mathbf{k}_{0\perp}|\equiv|k_{0x}\hat{\mathbf{x}}+k_{0y}\hat{\mathbf{y}}|\ ,$$

implying propagation nearly along a low-index crystal axis z and termed the cross-grating geometry (CGG); (2) $\mathbf{r}_\perp\equiv\mathbf{x}$,

$$|\mathbf{k}_{0\parallel}|\equiv|k_{0z}\hat{\mathbf{z}}+k_{0y}\hat{\mathbf{y}}|\gg|\mathbf{k}_{0\perp}|\equiv|k_{0x}|\ ,$$

implying propagation nearly along a low-index crystal plane y-z and termed the systematic-reflection geometry (SRG) (cf. Fig. 1). In both geometries, we shall refer to the direction(s) $\mathbf{r}_\perp$ as transverse and to $\mathbf{r}_\parallel||\mathbf{k}_{0\parallel}$ as longitudinal.

B. Iterative treatment of LVP effects

The longitudinal propagation of a fast particle is expected to be nearly free (i.e., only weakly affected by the LVP), whereas its transverse propagation can be strongly affected by the transverse variation of the potential. We

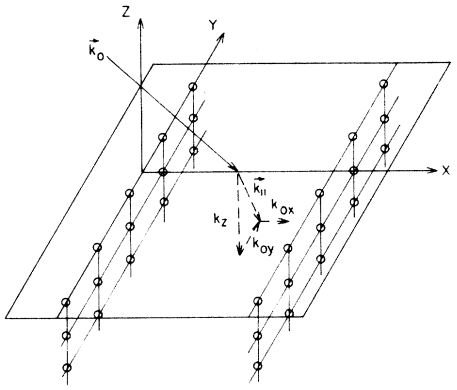

FIG. 1. Systematic-reflection geometry. The projections of the momentum of the incident particle on the crystal axes are shown.

therefore consider separately the equations governing transverse BC's (labeled by purely transverse $\mathbf{g}$'s) and those governing longitudinal BC's (labeled by RLV's with longitudinal components, hereafter denoted by $\mathbf{h}$), rewriting the set of equations (2) as the following two subsets:

$$[\epsilon_{\perp}^{(\mathbf{k})}-(k_{\perp}^2+D_{\mathbf{g}_{\perp}}^{(\mathbf{k}_{\perp})})]c_{\mathbf{g}_{\perp}}^{(\mathbf{k})}=\sum_{\mathbf{g}_{\perp}'\,(\neq 0)} U_{\mathbf{g}_{\perp}'}c_{\mathbf{g}_{\perp}-\mathbf{g}_{\perp}'}^{(\mathbf{k})} + \sum_{\mathbf{h}\,(\neq 0)} U_{\mathbf{g}_{\perp}-\mathbf{h}}c_{\mathbf{h}}^{(\mathbf{k})} , \tag{4a}$$

$$c_{\mathbf{h}}^{(\mathbf{k})}=\frac{1}{\epsilon_{\perp}^{(\mathbf{k})}-(k_{\perp}^2+D_{\mathbf{h}}^{(\mathbf{k})})}\left[\sum_{\mathbf{g}_{\perp}'} U_{\mathbf{h}-\mathbf{g}_{\perp}'}c_{\mathbf{g}_{\perp}'}^{(\mathbf{k})} + \sum_{\mathbf{h}'\,(\neq 0)} U_{\mathbf{h}-\mathbf{h}'}c_{\mathbf{h}'}^{(\mathbf{k})}\right] . \tag{4b}$$

The $c_{\mathbf{h}}^{(\mathbf{k})}$, expressing the longitudinal modulation of the eigenfunctions, exist due to the longitudinally varying parts of the potential. Here,

$$D_{\mathbf{g}_{\perp}}^{(\mathbf{k}_{\perp})}\equiv 2\mathbf{k}_{\perp}\cdot\mathbf{g}_{\perp}+g_{\perp}^2,\quad D_{\mathbf{h}}^{(\mathbf{k})}\equiv 2\mathbf{k}\cdot\mathbf{h}+h^2 , \tag{5a}$$

$$\epsilon_{\perp}^{(\mathbf{k})}-k_{\perp}^2\equiv k_0^2-U_0-k^2=k_{02}^2-U_0-k_z^2 , \tag{5b}$$

the last equality following from Eq. (3). The expression $\hbar^2\epsilon_{\perp}^{(\mathbf{k})}/2m\gamma$ [cf. Eq. (2b)] becomes the exact transverse energy eigenvalue upon ignoring LVP effects.[6–10] Since these effects are expected to be weak, it can still be approximately identified with the transverse energy. Hence, $\epsilon_{\perp}$ and k_z are restricted to bands of values allowed by the transverse periodicity of the potential.

The coefficients of $c_{\mathbf{g}}^{(\mathbf{k})}$ in Eq. (4b) can be simplified, upon use of Eqs. (2b), (3), and (5), as follows:

$$\frac{U_{\mathbf{h}-\mathbf{g}_{\perp}'}}{\epsilon_{\perp}^{(\mathbf{k})}-(k_{\perp}^2+D_{\mathbf{h}}^{(\mathbf{k})})}=-\frac{\phi_{\mathbf{h}-\mathbf{g}_{\perp}'}\chi_{\mathbf{h}}}{1-\kappa_{\mathbf{h}}^{(\mathbf{k})}+O(V/E)} . \tag{6}$$

A similar expression, with $\phi_{\mathbf{h}-\mathbf{h}'}$ replacing $\phi_{\mathbf{h}-\mathbf{g}'}$, is obtained for the coefficients of $c_{\mathbf{h}'}^{(\mathbf{k})}$. Here,

$$\phi_{\mathbf{g}}\equiv |\,V_{\mathbf{g}}/V_{g_m}\,| ,$$
$$\chi_{\mathbf{h}}\equiv\frac{\gamma V_{g_m}}{(\gamma^2-1)^{1/2}\hbar c(\hat{\mathbf{k}}_{0\parallel}\cdot\mathbf{h})} , \tag{7}$$
$$\kappa_{\mathbf{h}}^{(\mathbf{k})}\equiv[\epsilon_{\perp}^{(\mathbf{k})}-(\mathbf{k}_{\perp}+\mathbf{h})^2]/2\mathbf{k}_{0\parallel}\cdot\mathbf{h} ,$$

g_m being the shortest RLV corresponding to a nonzero structure factor and $\hat{\mathbf{k}}_{0\parallel}$ the longitudinal part of the unit vector in the direction of incidence.

For electrons and positrons (β particles) with $E_K\gtrsim 10$ keV and protons with $E_K\gtrsim 10$ MeV, we find that, both in the CGG and the SRG,

$$|\chi_{\mathbf{h}}|\lesssim|\kappa_{\mathbf{h}}^{(\mathbf{k})}|\ll 1$$

in a large variety of crystals. If these inequalities hold, then, in view of the fact that the $\phi_{\mathbf{g}}$ decrease with the modulus of $\mathbf{g}$ (and satisfy $|\phi_{\mathbf{g}}|\leq 1$ in many crystals),[44] the coefficients given by Eq. (6) are much smaller than 1 in absolute value. We may then apply an iterative process to Eqs. (4), increasing the accuracy by an order of $\chi_{\mathbf{h}}$ or $\kappa_{\mathbf{h}}^{(\mathbf{k})}$ in each iteration.

In the *first iteration* we keep only the leading terms in both Eqs. (4a) and (4b). Equation (4a) then yields the $c_{\mathbf{g}}^{(\mathbf{k})}$ upon neglect of the $c_{\mathbf{h}}^{(\mathbf{k})}$ (which are of order $\chi_{\mathbf{h}}$):

$$[\epsilon_{\perp}^{(\mathbf{k})}-(k_{\perp}^2+D_{\mathbf{g}_{\perp}}^{(\mathbf{k}_{\perp})})]c_{\mathbf{g}_{\perp}}^{(\mathbf{k})}=\sum_{\mathbf{g}_{\perp}'\,(\neq 0)} U_{\mathbf{g}_{\perp}'}c_{\mathbf{g}_{\perp}-\mathbf{g}_{\perp}'}^{(\mathbf{k})} . \tag{8a}$$

The Fourier components $U_{\mathbf{g}_{\perp}}$ governing the $c_{\mathbf{g}_{\perp}}^{(\mathbf{k})}$ constitute the projected potential.[12] The $c_{\mathbf{h}}^{(\mathbf{k})}$ are computed in the first iteration upon use of the $c_{\mathbf{g}}^{(\mathbf{k})}$ given by Eq. (8a) in Eq. (4b) and ignoring the $c_{\mathbf{h}'}^{(\mathbf{k})}$ therein, since their contributions are $O(\chi_{\mathbf{h}}^2)$.

In the *second iteration* we use the first-iteration results for the $c_{\mathbf{h}}^{(\mathbf{k})}$, in order to include the LVP corrections (to order $\chi_{\mathbf{h}}$) in Eq. (4a), as follows:

$$[\tilde{\epsilon}_{\perp}^{(\mathbf{k}')}-(k_{\perp}^2+D_{\mathbf{g}_{\perp}}^{(\mathbf{k}_{\perp})})]\tilde{c}_{\mathbf{g}_{\perp}}^{(\mathbf{k})}=\sum_{\mathbf{g}_{\perp}'\,(\neq 0)}\left[U_{\mathbf{g}_{\perp}'}-\sum_{\mathbf{h}\,(\neq 0)}\chi_{\mathbf{h}}\sum_{\mathbf{g}_{\perp}''}\phi_{\mathbf{g}_{\perp}'+\mathbf{g}_{\perp}''-\mathbf{h}}U_{\mathbf{h}-\mathbf{g}_{\perp}''}\right]\tilde{c}_{\mathbf{g}_{\perp}-\mathbf{g}_{\perp}'}^{(\mathbf{k})}+O(\chi_{\mathbf{h}}^2,\chi_{\mathbf{h}}\kappa_{\mathbf{h}}) . \tag{8b}$$

Thus the LVP-corrected transverse energies and BC's $\tilde{\epsilon}_{\perp}^{(\mathbf{k})},\tilde{c}_{\mathbf{g}}^{(\mathbf{k})}$ are obtainable from *the same set* of equations as the projection-approximation Eq. (8a), upon replacement of the projected-potential components in the latter equation by corrected components, given by the expressions in large parentheses on the right-hand side of Eq. (8b). The second-iteration form of the $c_{\mathbf{h}}^{(\mathbf{k})}$ is, as inferred from Eqs. (4b) and (8b),

$$c_{\mathbf{h}}^{(\mathbf{k})}=-\chi_{\mathbf{h}}\left[\sum_{\mathbf{g}_{\perp}'}\phi_{\mathbf{h}-\mathbf{g}_{\perp}'}\tilde{c}_{\mathbf{g}_{\perp}'}^{(\mathbf{k})}+\kappa_{\mathbf{h}}^{(\mathbf{k})}\sum_{\mathbf{g}_{\perp}'}\phi_{\mathbf{h}-\mathbf{g}_{\perp}'}c_{\mathbf{g}_{\perp}'}^{(\mathbf{k})}-\sum_{\mathbf{h}'\,(\neq 0)}\chi_{\mathbf{h}'}\phi_{\mathbf{h}-\mathbf{h}'}\sum_{\mathbf{g}_{\perp}'}\phi_{\mathbf{h}-\mathbf{g}_{\perp}'}c_{\mathbf{g}_{\perp}'}^{(\mathbf{k})}\right]+O(\chi_{\mathbf{h}}^2\kappa_{\mathbf{h}},\chi_{\mathbf{h}}^3,\chi_{\mathbf{h}}\kappa_{\mathbf{h}}^2) . \tag{8c}$$

The above scheme for the evaluation of $c_{\mathbf{h}}^{(\mathbf{k})}$ has been used before by Kurizki and McIver[28,30] in LM-emission calculations to first-iteration accuracy only. Vedrinskii and Malyshevskii[45] have derived, for the special case of LM emission from axially channeled particles, a formula of the same accuracy. However, as has been recently shown,[24] such accuracy is *inadequate* for LM-emission calculations. This can be understood upon inspection of the general form of a radiative-transition matrix element,[28]

$$\mathbf{M}_{if}^{(\mathbf{K})}=\frac{\hbar}{mc\gamma_i}\sum_{\mathbf{g}} c_{\mathbf{g}}^{(i)}c_{\mathbf{g}+\mathbf{K}}^{*(f)}(\mathbf{k}_i+\mathbf{g})\delta(\mathbf{k}_i-\mathbf{k}_f-\mathbf{K}-\mathbf{q}) ,$$

where i,f label the eigenstates before and after the emission, respectively, $\mathbf{K}$ is a RLV determining the momentum transfer to the crystal in the emission act, and $\mathbf{q}$ is the photon wave vector. LM emission is obtained if $\mathbf{K}_{||}\neq\mathbf{0}$. The component proportional to $\mathbf{k}_i$ in the LM matrix element can be shown to *vanish* if the first-iteration form of $c_{\mathbf{h}}^{(\mathbf{k})}$ is used. However, upon taking into account the second-iteration corrections to the $c_{\mathbf{h}}^{(\mathbf{k})}$ given by Eq. (8c), this component is found to produce, in certain cases, the *leading contribution* to LM-emission intensity.[24]

Buxton[16] has treated LVP effects using a basis of projected-potential eigenfunctions pertaining to all nonequivalent reciprocal-lattice layers within a unit cell in the z direction, and then considering the longitudinally varying part of the potential as a perturbation in this basis. In order to obtain a longitudinal BC using Buxton's approach, one must perform (even to first-iteration accuracy) toilsome summations over *all* transverse energy bands of all the different layers and all longitudinal RLV's. The present treatment is much less time-consuming and simpler, since it does not involve summations over different layers or transverse energy bands, and yields directly the longitudinal BC's for each *specific* value of the transverse energy. This association of the longitudinal BC's with a specific transverse energy is required for the evaluation of $\mathbf{M}_{if}^{(\mathbf{K}_{||}\neq\mathbf{0})}$ (see above), since i,f are associated with specific transverse energies.

It can be shown[24] that the LVP corrections contained in the $\tilde{c}_{\mathbf{g}_\perp}^{(\mathbf{k})}$ [cf. Eq. (8b)] do not contribute to LM emission to second-iteration accuracy. Therefore, the $c_{\mathbf{g}_\perp}^{(\mathbf{k})}$ and $\epsilon_\perp^{(\mathbf{k})}$ obtainable from Eq. (8a), which suffice to calculate [from Eq. (8c)] the parts of $c_{\mathbf{h}}^{(\mathbf{k})}$ relevant to LM emission, constitute the required input for the evaluation of all types of $\mathbf{M}_{if}^{(\mathbf{K})}$.

In what follows the analysis of Eq. (8a) will be restricted to the SRG, which allows the application of the powerful Hill's-equation method. The purpose will be to investigate those effects of the projected-potential periodicity that are presently obtainable only numerically [i.e., by solving Eq. (8a) using "many-beam" methods[6,7,37–39]].

III. HILL'S-EQUATION ANALYSIS: PRELIMINARIES

We transform Eq. (8a) in the SRG to the coordinate representation and thus obtain the one-dimensional Schrödinger-type equation:

$$\left[\frac{d^2}{dx^2}+\epsilon_x-\bar{U}(x)\right]w(x)=0 , \tag{9a}$$

where

$$\epsilon_x\equiv\epsilon_\perp ,$$
$$\bar{U}(x)\equiv\sum_{g_x} U_{g_x}e^{ig_x x} , \tag{9b}$$
$$w(x)=\sum_{g_x} c_{g_x}e^{i(k_x+g_x)x} .$$

Because the parameter $\bar{U}(x)$ is periodic in x, Eq. (9a) is of the type known as Hill's equation.[46]

In order to make the treatment both simpler and more informative, we shall henceforth restrict ourselves to centrosymmetric sets of systematic reflections, for which $U_{g_x}=U_{-g_x}$, all U_{g_x} being real. This condition confines us to all reflections in centrosymmetric crystals and to certain reflections in other crystals.[44] With this condition in mind, Eq. (9a) can be transformed to the following dimensionless form:

$$w''+\left[\lambda+2\sum_j \theta_j\cos(2j\xi)\right]w=0 , \tag{10a}$$

where

$$(\ )'=\frac{d}{d\xi}(\ ),\quad \xi=(g_x)_{\min}x/2 , \tag{10b}$$

$$\theta_j=-U_j/(g_x/2)_{\min}=-\gamma V_j/E_B,\quad E_B=\hbar^2(g_x)_{\min}^2/8m .$$

Here, $(g_x)_{\min}$ is the shortest RLV of the systematic-reflection set g_x. The origin of ξ is at the center of symmetry.

The following abbreviations will be used henceforth:

$$q(\xi)=-2\sum_j \theta_j\cos(2j\xi),\quad f(\xi)=\lambda-q(\xi) . \tag{11}$$

The potential function $q(\xi)$ has a period π in terms of ξ [i.e., $q(0)=q(\pi)$]. In the range $0\le\xi\le\pi$, $\xi_{\max}$ and $\xi_{\min}$ will denote the positions of the highest maximum and lowest minimum of $q(\xi)$, respectively.

The potential Fourier coefficients V_j, and thus also the θ_j, are proportional to the crystal structure factor:[44]

$$\theta_j\propto\mathscr{S}_j=\sum_p (F_j)_p\exp[i(g_x)_{\min}jx_p] , \tag{12}$$

where x_p stands for the position of the pth atom in the unit cell and $(F_j)_p$ is the atomic scattering factor (form factor) associated with the pth atom and the RLV $(g_x)_{\min}j$. It is easily shown that

$$\theta_j^{\pm}=\mp|\theta_j|\,\mathrm{sgn}\mathscr{S}_j . \tag{13}$$

Here and hereafter the $+,-$ superscripts on potential and eigenvalue parameters refer to positive and negative particles, respectively.

In the case of a single potential-minimum located at the center of the unit cell,[44] it is advantageous to choose $\xi_{\max}^{\pm}=0$ for both positive and negative particles. This requires the following coordinate shift of the potential curve

[Eq. (11)] for negative particles with respect to that for positive particles: $\xi \rightarrow \xi + \pi/2$. We then have, in the single-minimum case,

$$\theta_j^+ = -|\theta_j| \operatorname{sgn}\mathscr{S}_j, \quad \theta_j^- = (-1)^j |\theta_j| \operatorname{sgn}\mathscr{S}_j . \quad (14a)$$

The "depth" of the potential function (the difference between its maximum and minimum) in this case is given by

$$q^{\pm}(0) - q^{\pm}(\pi/2) = 4 \sum_k |\theta_{2k-1}| \operatorname{sgn}\mathscr{S}_{2k-1} . \quad (14b)$$

In fcc and bcc lattices, by choosing $(g_x)_{\min}$ such that $\mathscr{S}_j \neq 0$ for all j ($j = 1,2,\ldots$), Eqs. (14) are reduced to a simple form with $\operatorname{sgn}\mathscr{S}_j = 1$ identically.

Using the relativistic Hartree-Fock model of Doyle and Turner,[47] we find that the F_j in Eq. (12) satisfy

$$F_j \propto (m\gamma/m_e) \sum_{i=1}^{4} a_i e^{-[b_i (g_x)_{\min}^2 j^2 + a_T^2/2]} . \quad (15)$$

Here, a_i and b_i are constants that characterize the atomic scattering factor for electrons, $m\gamma/m_e$ is the ratio of the relativistic mass of the particle to the electron rest mass, and a_T is the temperature-dependent amplitude of thermal vibrations which enters into the exponent of the Debye-Waller factor. It is clear that for sufficiently large j, such that the expression in square brackets is much greater than unity for all four values of b_i, the $|\theta_j|$ tend to zero very rapidly. Hence, the important convergence condition

$$\sum_j |\theta_j| j^n < \infty , \quad (16)$$

where n is any integer, is satisfied. It allows truncation of all the j summations in all the formulas in this text above $j = j_{\max}$. Here, $j_{\max}$, corresponding to the desired accuracy, is chosen as follows:

$$|\theta_{j_{\max}}| / |\theta_1| \simeq 10^{-2} . \quad (17)$$

According to Eq. (15), $|\theta_j|$ and $j_{\max}$ depend very strongly upon $(g_x)_{\min}^2$ for a given set of atomic and thermal parameters. Thus, we find that, for many fcc crystals with $a_T \simeq 0.1$ Å, incidence nearly along a (101) plane implies $j_{\max} = 4$, as compared to $j_{\max} = 7$ for incidence along a (111) plane.

It follows from the above discussion that the ratios $\phi_j^{\pm} = \theta_j^{\pm} / |\theta_1|$ [cf. Eq. (7)] are fixed once the crystal, temperature, and direction of incidence [i.e., $(g_x)_{\min}$] have been specified. The information on the strength of $q(\xi)$ is in $|\theta_1|$, whose magnitude plays a crucial role in determining the nature of Hill's-equation solutions. The proportionality of $|\theta_1|$ to γ [Eq. (2b)] is determined from Eqs. (10b), (12), and (15). For electrons or positrons (β particles) $|\theta_1|$ can range from values smaller than 0.1γ [e.g., for fcc crystals with atomic numbers less than 30 and incidence along (101) planes] and up to γ [e.g., for fcc crystals with high atomic numbers and incidence nearly along (111) planes]. For both π mesons and protons, $|\theta_1| \gg \gamma$.

In what follows we shall analyze Hill's equation for two ranges of $|\theta_1|$ values, which, in view of the above discussion, can be characterized as follows:

(1) The "shallow-potential" situation $|\theta_1| < 1$, which may occur only for β particles with energies less than 5 MeV.

(2) The "deep-potential" situation $|\theta_1| \gg 1$, which is almost always the case for β particles with energies above 50 MeV (except for incidence along planes with rather high indices) and for all heavier fast particles.

In order to deal with the boundary conditions imposed by the incident plane wave $\exp(ik_{0x}x)$, we introduce the following definition:

$$k_{0x}/(g_x/2)_{\min} \equiv l \equiv [l] + \mu , \quad (18)$$

where $[l]$ is the largest integer not exceeding l, and μ ($0 \leq \mu \leq 1$) measures the deviation of the incident wave $\exp(il\xi)$ from the lth Bragg angle. The general properties of the solutions of Hill's equation[46] imply that (1) the fractional part of the characteristic exponent of the eigenfunctions must be equal to μ, and (2) incidence at a Bragg angle (i.e., $l = [l]$) induces either π-periodic or 2π-periodic eigenfunctions (associated with eigenvalue band edges), according to whether l is even or odd, respectively.

For any form of the solutions, l determines the probability of exciting (populating) the nth eigenstate $w_n(\mu,\xi)$. Neglecting the elastically backscattered waves (which are very weak for incidence angles less than $\sim 80°$ with respect to the z axis[6]), as well as the contributions of longitudinal BC's given by Eq. (8c), this probability $P(n,\mu)$ is found from

$$P(n,\mu) = \pi^{-2} \left| \int_0^{\pi} w_n(\mu,\xi) e^{-il\xi} d\xi \right|^2 . \quad (19)$$

IV. THE "SHALLOW-POTENTIAL" SITUATION

A. Large angles of incidence: The kinematic regime

In the limit of large-index eigenvalues (corresponding to high levels of transverse energy) of the $|\theta_1| < 1$ situation, the asymptotic expressions for the eigenvalues are [cf. Eqs. (10) and (11)]:[48]

$$\lambda_{2r}^{(\pi)} \simeq \lambda_{2r-1}^{(\pi)} = 4r^2 + \frac{1}{32\pi r^2} \int_0^{\pi} q^2(\xi) d\xi + O(1/\lambda^2) ,$$
$$\lambda_{2r-1}^{(2\pi)} \simeq \lambda_{2r}^{(2\pi)} = (2r-1)^2 + \frac{1}{32\pi r^2} \int_0^{\pi} q^2(\xi) d\xi + O(1/\lambda^2) , \quad (20)$$

where $\lambda^{(\pi)}, \lambda^{(2\pi)}$ denote the eigenvalues of π-periodic and 2π-periodic solutions, respectively. The approximate equality signs suggest that the forbidden energy gaps[46] are extremely narrow in this limit.

The "normalized" even and odd solutions[46] y_e and y_o, from which the eigenfunctions are to be constructed in this limit, are given by Eqs. (A1) and (A2).[49] The application of the boundary conditions [Eqs. (18) and (19)] for an incident $\exp(il\xi)$ wave ($|l| \gg 1$) to these solutions shows that the eigenfunction associated with

$$\lambda = l^2 + \int_0^{\pi} q^2(\xi) d\xi / 8\pi [l]^2 ,$$

namely

$$w_\lambda(\xi)=y_e(\lambda,\xi)+ily_o(\lambda,\xi)$$
$$=\exp(il\xi)+O(|\theta_1|/l)\,, \tag{21}$$

is the only one that is strongly excited, i.e., populated with probability $1-O(\theta_1^4/l^2)$. When $l=2r$, only $y_{e,o}(\lambda_{2r}^{(\pi)},\xi)$ are excited, whereas $y_{e,o}(\lambda_{2r-1}^{(2\pi)},\xi)$ only are excited for $l=2r-1$. No Bragg reflections occur in this limit, the only "strong-beam" coefficient being that of $\exp(il\xi)$.

The potential effects amount here to a weak perturbation of the incident plane wave, which is described by Eqs. (20), (A1), and (A2) to the same degree of accuracy as the second Born approximation. The advantage of the present formalism is that both the potential effects and the boundary conditions are contained in the solutions, thus making the formulas more concise. It also allows unification of the treatment of this regime with that of other regimes.

B. Smaller angles of incidence: Dynamical diffraction

One of the features of dynamical diffraction is the emergence of a distinct energy-band structure, or, equivalently, the appearance of appreciable gaps in the energy spectrum.[50,51] In the "shallow-potential" situation, the width of the nth band gap in the transverse energy spectrum[52] is of the order of $|\theta_1|$ for $n<j_{\max}$ [Eq. (17)], then drops down to $\sim|\theta_{j_{\max}}|\sim 10^{-2}|\theta_1|$ for $n=j_{\max}$, and becomes negligible for $n\geq 2j_{\max}$. We may therefore conclude that the kinematic treatment is certainly appropriate for $n\geq 2j_{\max}$ and, to a good approximation, even for $n\geq j_{\max}$, whereas for the first several bands dynamical diffraction of the incident wave may take place.

Solutions appropriate for low band-indices have been given in a detailed form by Ince.[53,54] Ince's approximations for the eigenvalues can be written to first order in θ_j as follows:

$$\lambda_{n=0}^{(1)}=\mu^2,\quad \lambda_{n\neq 0}^{(1)}=n^2+\theta_n^{\pm}\cos(2\sigma_n^{(1)})\,, \tag{22a}$$

where the parameter σ is a complex quantity which may be defined for stable (allowed) solutions,[25] to the same accuracy, as

$$\sin(2\sigma_{n\neq 0}^{(1)})\simeq 2ni\mu/\theta_n^{\pm}\,. \tag{22b}$$

A stable Ince's solution $y_n(\mu,\xi)$ can be written to first order in $|\theta_j|$ as [cf. Eqs. (A3) and (A4) for details]

$$y_{n=0}^{(1)}(\mu,\xi)=e^{i\mu\xi}\left[1+\sum_{j=1}^{j_{\max}}O(\theta_j)e^{\pm i2j\xi}\right],$$
$$y_{n\neq 0}^{(1)}(\mu,\xi)=e^{i\mu\xi}\left[\sin(n\xi-\sigma_n)+\sum_{j=1}^{j_{\max}}O(\theta_j)e^{\pm i(2j\pm n)\xi}\right]. \tag{23}$$

Although the eigenfunction $w_n(\mu,\xi)$ should, in principle, contain a term that is proportional to $y_n(-\mu,-\sigma_n,\xi)$,[54] we can show that the boundary condition [Eq. (18)] implies in this case

$$w_n(\mu,\xi)=\left[\pi^{-1}\int_0^{\pi}|y_n(\mu,\xi)|^2d\xi\right]^{-1/2}y_n(\mu,\xi)\,. \tag{24}$$

For $\mu=0$ the eigenfunction becomes periodic (π periodic for n even, 2π periodic for n odd). Then $w_n(0,\xi)$ is even for $\sigma_n=\pi/2$ and odd for $\sigma_n=0$.

It is readily seen from Eq. (23) that when $\mu=0$ the coefficients of the leading harmonic $\exp(\pm in\xi)$ acquire the same magnitude. This marks the occurrence of the nth Bragg reflection, which is caused by the incidence of a $\exp(in\xi)$ wave. Only two "strong beams" may be simultaneously excited in $w_n(\xi)$ in this regime. The coefficients of the "weak beams,"

$$\exp\{i[\mu\pm(2j\pm n)]\xi\}\,,$$

represent the total projected-potential perturbative effect on the incident and reflected waves.

The basis difference between Ince's eigenfunctions and those given by Eq. (21) lies in the form of the leading harmonics. In the latter case, these are of the form $\exp[i(\mu+n)\xi]$, which produce only running waves that are uniformly spread transversely to the crystalline planes. In the former case, $\exp[i(\mu+n)\xi]$ and $\exp[i(\mu-n)\xi]$ can combine to yield a standing wave at a Bragg angle. Such a wave is spatially localized either at the atomic planes bordering the unit cell or halfway between them [depending on the parity of $w_n(\xi)$ and the charge sign]. This difference between the solutions in the two regimes is related to the fact that in the limit of high transverse energies μ is part of the eigenvalue l^2, which varies *continuously* with $l=n+\mu$, whereas for low-index bands μ is related to λ indirectly through σ, thus leading to *discontinuities* in the transverse energy. An analogous state of affairs will recur in the "deep-potential" situation.

The width of the gaps separating the bands described by Eqs. (22) is equal, to lowest order, to $2|\theta_n|$. The lower edge ($\mu=0$) of the lowest ($n=0$) band can be shown from Eq. (22a) to be situated below the barrier (Fig. 2) irrespective of the magnitude of $|\theta_j|$. The condition for the lower edge of the nth band to be located below the barrier is [cf. Eqs. (22) and (11)]:

$$n^2+|\theta_n|<-2\sum_j\theta_j^{\pm}\cos(2j\xi_{\max}^{\pm})\,. \tag{25}$$

The right-hand side of Eq. (25) is always positive for fcc and bcc lattices. However, even in that case it can be just

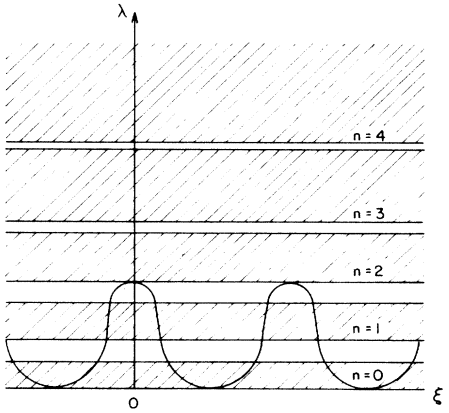

FIG. 2. Band structure for positrons in a shallow potential. Allowed (stable) transverse energy bands are shaded. The top of the $n=1$ band is shown to lie below the potential barrier.

barely satisfied for $n=2$ (and not at all for $n>2$) without violating the condition $|\theta_1|<1$, which is necessary for the validity of Ince's approximation. For fcc and bcc lattices,

$$\left|\sum_j \phi_j^+\right| > \left|\sum_j \phi_j^-\right| ;$$

hence, positive particles are more likely to be trapped by the "shallow potential." The explanation for this phenomenon can be found in Fig. 2. Because the potential for positive particles is more strongly cusped near the maxima, as compared to that for negative particles, it is more likely to confine the motion of a particle with energy in the vicinity of the barrier energy.

The approximations discussed above can be used, instead of numerical "many-beam" calculations,[6-7] for a reasonably accurate analytical evaluation of matrix elements for *all types* of radiative transitions in the shallow potential: (a) interband transitions, in which n_i-n_f corresponds to K_x momentum transfer (cf. Sec. II B); (b) intraband transitions ($n_i=n_f$) across the band gap $2|\theta_{n_i}|$; (c) LM transitions, involving either $n_i=n_f$ or $n_i\neq n_f$.

V. THE "DEEP-POTENTIAL" SITUATION

A. Unbound (above-the-barrier) states

We shall seek to obtain a more accurate description of unbound states than what is presently used in this field. The commonly used[12] lowest-order Wentzel-Kramers-Brillouin (WKB) solutions in this case, which implies $f(\xi)>0$ for all ξ [cf. Eq. (11)], are the travelling waves:[55,56]

$$y_\pm(\xi)=A\exp\left[\pm i\int_0^\xi f^{1/2}(\xi)d\xi\right]\Big/f^{1/4}(\xi) ,$$
$$A=\left[\int_0^\pi f^{-1/2}(\xi)d\xi\right]^{-1/2} . \quad (26)$$

In the exponent of $y_\pm(\xi)$ in Eq. (26), terms smaller than $|\theta_1|^{1/2}$ are neglected. Such terms, however, become important for $|\theta_1|\lesssim 10^4$ (which is typically the case with β particles below 1 GeV, nonrelativistic protons, and pions). Therefore, for moderately large values of $|\theta_1|$ we adopt an ameliorated solution using an iteration procedure[55] which allows the calculation of the $(r+1)$th-order exponent for $y_\pm(\xi)$ from the exponent obtained after the rth iteration [$f^{(0)}(\xi)\equiv f(\xi)$].

It can be shown by induction that $[f^{(r)}(\xi)]^{1/2}$ contains terms as small as

$$(|\theta_1|/\lambda)^{2r}\lambda^{-r+1/2}<|\theta_1|^{-r+1/2} .$$

If an accuracy of 1% is sought, it then follows that we need $r\lesssim 2/\log_{10}|\theta_1|-\frac{1}{2}$. We shall be content with using $[f^{(1)}(\xi)]^{1/2}$ in subsequent calculations, thereby making the treatment accurate within 1% for $|\theta_1|\gtrsim 30$ (which is typically the case with β-particle energies above 100 MeV or at most 300 MeV). This changes the integrand in the exponent of Eq. (26) to[55]

$$\tilde{f}^{1/2}(\xi)\equiv[f^{(1)}(\xi)]^{1/2}=f^{1/2}(\xi)+\delta f(\xi) , \quad (27a)$$

where

$$\delta f=\frac{f''}{8f^{3/2}}-\frac{5(f')^2}{92f^{5/2}}=|\theta_1|\frac{\sum_{j=1}^{j_{\max}}\phi_j^\pm j^2\cos(2j\xi)}{\lambda^{3/2}[1-q(\xi)/\lambda]^{3/2}}-\frac{5\theta_1^2}{2\lambda^{5/2}[1-q(\xi)/\lambda]^{5/2}}\sum_{j=1}^{j_{\max}}\sum_{j'=1}^{j_{\max}}jj'\phi_j^\pm\phi_{j'}^\mp\sin(2j\xi)\sin(2j'\xi) . \quad (27b)$$

The corresponding approximate form for above-the-barrier eigenfunctions, anticipating the result expressed in Eq. (31a), is

$$w_n(\xi)\simeq A^{(n)}\tilde{f}^{-1/4}(\xi)\exp\left[\pm i(\mu+n)\int_0^\xi \tilde{f}_n^{1/2}(\xi)d\xi/\tilde{\beta}_n\right] . \quad (28a)$$

Here, $\tilde{\beta}_n$ is the closed-orbit action integral $\oint p\,dx$,[56] given in our notation by

$$\tilde{\beta}_n=\pi^{-1}\int_0^\pi \tilde{f}_n^{1/2}(\xi)d\xi . \quad (28b)$$

The above-the-barrier eigenfunctions resemble the "large-angle" (kinematic limit) eigenfunctions in that both represent running waves as opposed to Ince's solutions: the latter form standing waves at the Bragg incidence angles. A comparison between Eqs. (28) and Eqs. (21) and (23) shows that the role of the phase $(\mu+n)\xi$ in the shallow-potential situation has been assumed by the phase integral $[(\mu+n)/\tilde{\beta}_n]\int_0^\xi \tilde{f}_n^{1/2}(\xi)d\xi$ in the deep-potential situation. This suggests that the many harmonics $\exp(\pm i2j\xi)$ contained in $\tilde{f}_n(\xi)$ can significantly affect the behavior of the eigenfunction in the deep-potential situation, so that $w_n(\xi)$ associated with bands not too high above the barrier should consist of many beams of comparable strength.

This expectation can be confirmed by an explicit analytic evaluation of the eigenfunctions. Since $\lambda>q(\xi_{\max})$ [Eq. (11)] for above-the-barrier states, the square root $[f^{(r)}(\xi)]^{1/2}$ can be expanded in powers of $q(\xi)/\lambda\propto 2|\theta_1|/\lambda$. The terms of the expansion are proportional to powers of $\sum_j\phi_j^\pm\cos(2j\xi)$ and derivatives thereof, and therefore the integration of the expansion to obtain the exponent of the eigenfunction, $i\int_0^\xi[f^{(r)}(\xi)]^{1/2}d\xi$, is straightforward:[57]

$$\exp\left[\pm i(\mu+n)\int_0^{\xi} d\xi\,\tilde{f}_n^{1/2}(\xi)/\tilde{\beta}_n\right]=\exp[\pm i(\mu+n)\xi]\prod_{j=1}^{j_{\max}}\left[J_0(Z_j^{(\mu,n)})+2\sum_{k=1}^{\infty}J_{2k}(Z_j^{(\mu,n)})\cos(4kj\xi)\right.$$
$$\left.\pm 2i\sum_{k=1}^{\infty}J_{2k+1}(Z_j^{(\mu,n)})\sin[(2k+1)2j\xi]\right]\exp[iO((|\theta_1|/\lambda)^2)]\,, \tag{29a}$$

where the J's denote Bessel functions, $j_{\max}$ is defined in Eq. (17) and $Z_j^{(\mu,n)}$ is defined as

$$Z_j^{(\mu,n)}=(\mu+n)(1-1/\tilde{\beta}_n\lambda_n^{1/2})\,|\theta_1|\,\phi_j^{\pm}/2\lambda_n j\,. \tag{29b}$$

Terms of each higher order in $|\theta_1|/\lambda$ can be expanded analogously in terms of Bessel functions, but the work involved in their evaluation will increase with the order m, since they will contain m multiple product series in $j, j', \ldots$ in lieu of the first-order single-product series.[58]

The character of the expression in Eq. (29a) is determined by the magnitude of $Z_1^{(\mu,n)}$. Again using the result $\lambda_n\simeq\pi^2n^2$ to be discussed later, we may estimate Z_1 in terms of the ratio $R=\lambda_n/|\theta_1|$. Such an estimate yields $Z_1\simeq(|\theta_1|/R/2\pi)^{1/2}$ For $R\geq 10$, which allows us to approximate the exponential of i times higher orders in $|\theta_1|/\lambda$ by 1, we may have either $Z_1\gg 1$ (this will commonly occur for $|\theta_1|\gg 10^3$, i.e., for β particles with energies well above a GeV or relativistic protons), or $Z_1<1$ (this is likely to occur for $|\theta_1|\lesssim 10^2$, i.e., for β particles with energies up to a few hundred MeV). Still, even for very large $|\theta_1|$, the limit $Z_1\ll 1$ will be attained for $2\pi^2n\gg|\theta_1|$ (see below).

For $Z_1\gg 1$ we have[57]

$$J_p(Z_j)=(2/\pi Z_j)^{1/2}\cos(Z_j-\pi p/2-\pi/4),\quad p=0,1,2,\ldots\,.$$

Hence, the coefficients of many of the various harmonics $\cos(4kj\xi)$, $\sin[(2k+1)2j\xi]$ in Eq. (29a) are roughly of the same magnitude, and $w_n(\xi)$ is expected to exhibit a strong many-beam character in this case. No drastic enhancement of particular beams occurs, as Bragg reflections are absent.[59]

For $Z_1<1$ and $R\gtrsim 10$, we find[57]

$$\exp\left[\pm i(\mu+n)\int_0^{\xi}\tilde{f}_n^{1/2}(\xi)d\xi/\tilde{\beta}_n\right]\simeq\exp[\pm i(\mu+n)\xi]\sum_{j=1}^{j_{\max}}\left[1\pm i(\mu+n)(1-1/\tilde{\beta}_n\lambda_n^{1/2})\frac{|\theta_1|}{2\lambda_n}\frac{\phi_j^{\pm}}{j}\sin(2j\xi)\right]. \tag{30}$$

Thus, sufficiently high above the barrier, where $2\pi^2n\gg|\theta_1|$, the eigenfunctions reduce to the form of weakly perturbed plane waves, similar to the kinematic-limit states in the shallow-potential situation.

While the corrections $\delta f(\xi)$ [Eq. (27b)] to the eigenfunctions in this regime have no qualitative significance, their effect on the eigenvalue spectrum is much more marked. The allowed unbound eigenvalues λ_n can be conveniently expressed as follows:[60]

$$\lambda_n^{1/2}\simeq\pi n\left[\int_0^{\pi}\left[1-\frac{q(\xi)}{2\pi(n+\mu)}\right]^{1/2}d\xi\right]^{-1}+L_n\cos(2\sigma_n)\,, \tag{31a}$$

where $n=2r+\mu$, and

$$L_n\sin(2\sigma_n)=2ni\mu,\quad |L_n|\simeq\frac{2n}{\pi}\left|\int_0^{\pi}\delta f_n(\xi)d\xi\right|. \tag{31b}$$

We see from Eq. (31a) that in the unbound regime, n is even for π-periodic states ($\mu=0$) and odd for 2π-periodic states ($\mu=1$). Equation (31b) shows that, in analogy to Ince's solutions [cf. Eqs. (22)], energy gaps of width $2L_n$ emerge, due to the correction $\delta f(\xi)$ (Fig. 3). It is easy to show that $L_n\propto(\theta_1/\lambda_n)^2\propto\theta_1^2/n^4$. The kinematic regime of Sec. IV A is retrieved when $|\theta_1|/2\pi^2n\ll 1$ [cf. Eq. (30)].[61]

The significance of the above gaps is revealed when computing the emission frequencies for unbound-unbound transitions.[30] It is then found that these frequencies deviate from the pure coherent bremsstrahlung frequency[31] [which is obtained in the kinematic regime, i.e., upon ignoring the L_n term in Eq. (31a)] by the factors $\pm(|L_{n_i}|\pm|L_{n_f}|)/(n_i-n_f)$, where, as in Sec. II B, i and f label the initial and final eigenstates. These deviations, which are not accounted for by the prevailing models,[31-33] introduce a rich structure into the spectrum of unbound transitions.

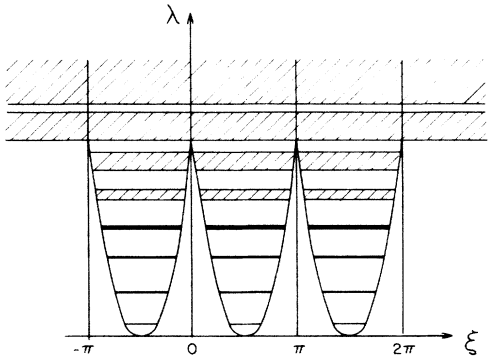

FIG. 3. Single-minimum deep potential for positive particles. Allowed transverse energy bands are shaded near the potential barrier and above it, marked by bold lines well below the barrier, and by thin lines (negligible bandwidth) near the bottom of the potential.

B. The channeling regime in a single-minimum potential

We turn now to the case in which the potential has a single minimum and $f(\xi)$ [Eq. (11)] has two simple zeros in a π period, corresponding to bound states, i.e., to transverse energies below the potential maxima. The bound regime in a single-minimum potential has been extensively investigated by Berry[12] with an emphasis on the transition to the classical picture of channeling trajectories. Our goals in considering this regime are to elucidate the points which have not been analyzed hitherto in detail, namely (a) the eigenvalue band structure and (b) tunneling into classically forbidden regions.

Instead of Berry's solutions, in which the penetration into classically forbidden regions is ignored, here we shall employ improved WKB eigenfunctions[62] in which there is a nonvanishing (albeit small) component that persists throughout the entire ξ space. These eigenfunctions [Eqs. (B1) and (B6)] allow the determination of the bandwidth imposed by the periodicity of the potential on the transverse energy levels.

The penetration of the nth-band eigenfunction into a classically forbidden region, e.g., the region $0<\xi<\alpha_1$, is governed by the factor

$$\exp\left[-\beta_2^{(n)}+\int_{\xi}^{\alpha_1^{(n)}}|\tilde{f}_n(\xi)|^{1/2}d\xi\right]\Big/|\tilde{f}_n(\xi)|^{1/4}, \tag{32a}$$

where

$$\beta_2^{(n)}=\int_{\alpha_2^{(n)}}^{\alpha_1^{(n)}}|\tilde{f}_n(\xi)|^{1/2}d\xi \tag{32b}$$

is the action associated with the potential crest, and $|\tilde{f}_n(\xi)|^{1/2}$ is given by Eqs. (27). For the WKB approximation to hold, we need $\beta_2^{(n)}$ to be considerably larger than 1. However, we shall see that even with this condition appreciable tunneling and bandwidth effects emerge in the bound regime.

The allowed transverse energies λ_n are obtained from the quantization condition on the action associated with the potential trough:

$$\beta_1^{(n)}=\int_{\alpha_1^{(n)}}^{\alpha_2^{(n)}}\tilde{f}_n^{1/2}(\xi)d\xi=(n+\tfrac{1}{2})\pi-\delta_n, \tag{33a}$$

where the parameter

$$\delta_n=(-1)^n\cos(\mu\pi)e^{-\beta_2^{(n)}} \tag{33b}$$

causes the nth band to be of the width

$$|\delta_n(\mu=0)-\delta_n(\mu=1)|=2e^{-\beta_2^{(n)}}. \tag{34}$$

In order to obtain explicit expressions for the *low-lying bands,* we require their turning points to be situated close to the potential minimum:

$$\alpha_1^{(n)}=\pi/2-\kappa_n,\quad \alpha_2^{(n)}=\pi/2+\kappa_n,\quad \kappa_n\ll 1. \tag{35}$$

This requirement [which will be shown to hold as long as Eq. (39) is satisfied] allows expansion of the integrand in Eq. (33a) in powers of $\delta\xi=\xi-\pi/2$. Defining

$$\Delta\lambda_n^{\pm}=\lambda_n^{\pm}-q^{\pm}(\pi/2), \tag{36}$$

where $q^{\pm}(\pi/2)$ [cf. Eqs. (11) and (14)] is the minimum of the potential function, we obtain for $f_n(\xi)$ the following expansion:

$$f_n(\pi/2+\delta\xi)=\Delta\lambda_n+4\left[b^{\pm}\delta\xi^2+\sum_{j=1}^{j_{\max}}(-1)^j\frac{\theta_j^{\pm}}{3}j^4\delta\xi^4+\cdots\right], \tag{37a}$$

$$b^{\pm}=\sum_{j=1}^{j_{\max}}(\mp 1)^{j+1}j^2|\theta_j|\,\mathrm{sgn}\mathscr{S}_j. \tag{37b}$$

Upon substitution of this expansion into Eqs. (32) and (33), we can obtain the anharmonic transverse energy spectrum (including bandwidth corrections) for low-lying bands of both negative and positive particles.

For positive particles the $\delta\xi^2$ contribution in Eq. (37a) predominates. Hence, upon neglect of the higher-power contributions, we obtain, from Eqs. (33a) and (35),

$$\Delta\lambda_n^{+}\simeq 4b^{+}\kappa_n^2=4(b^{+})^{1/2}(n+\tfrac{1}{2}). \tag{38}$$

The parameter $4(b^{+})^{1/2}$ corresponds to the frequency of oscillation in this harmonic-oscillator approximation. The requirement $\kappa_n\ll 1$ [Eq. (35)], on which this approximation is contingent, is seen from Eq. (38) to be equivalent to

$$n\ll(b^{+})^{1/2}\propto|\theta_1|^{1/2}\propto\gamma^{1/2}. \tag{39}$$

The harmonic-oscillator approximation for the eigenvalues can be obtained by a more formal method, consisting of an extension to Hill's equation (with $|\theta_1|\gg 1$, $\lambda<2|\theta_1|$) of a proof given in the literature for Mathieu's equation.[63] This method, which is free of the inherent limitation of the WKB method on the minimum spacing of the turning points[56]

$$2\kappa_n\simeq 2(b^{\pm})^{-1/4}(n+\tfrac{1}{2})^{1/2},$$

ensures the validity of Eq. (38) for all low-lying n, $n=0$ included. It also confirms the intuitively expected result that for low-lying bands of positive particles the $w_n(\xi)$ reduce approximately to the following superposition of parabolic-cylinder (harmonic-oscillator) functions D_n:[64]

$$w_{n,\mu}(\xi)\simeq w_{n,\mu}(\xi)_{\mathrm{harm}}=\sum_{m=-\infty}^{\infty}e^{i\mu m\pi}D_n((4b^{\pm})^{1/4}[\xi-(m+\tfrac{1}{2})\pi]). \tag{40}$$

The μ dependence of these Bloch waves causes them to lack definite parity unless the particle is incident at a Bragg angle ($\mu=0,1$). Hence (for $\mu\neq 0,1$) they allow dipolar radiative transitions

$$\int_{-\pi/2}^{\pi/2}d\xi\, w_{n_f,\mu}^{*}(dw_{n_i,\mu}/d\xi),$$

with $n_i-n_f=2$, whereas the single-well harmonic-oscillator eigenfunctions used by Kumakhov and Wedell[65] forbid such transitions. The cross section for the $2\rightarrow 0$ transition can be shown[66], using Eq. (40), to be smaller by

$$16\pi(b^{+})^{1/2}[2+\pi^2(b^{+})^{1/2}/2]^2\exp[-\pi^2(b^{+})^{1/2}/2]$$

than that of the fundamental $1\rightarrow 0$ transition (anharmonic corrections [cf. Eq. (41b)] do not change this ratio considerably). For $b^+ \lesssim 10$, this ratio is approximately greater than 10^{-2}, and hence the projected-potential periodicity has then a non-negligible effect even on the low-lying channeling states.

The above form of the eigenfunctions may be used to calculate the effects of anharmonicity for positive particles. Treating the $\delta\xi^4$ term in Eq. (37a) as a small perturbation, we take its expectation value with respect to the D_n and thus find the quartic anharmonic correction to the eigenvalues to be

$$(\Delta\lambda_n)^+_{\text{anh}} - (\Delta\lambda_n)^+_{\text{harm}} \simeq \sum_{j=1}^{j_{\max}} \frac{|\theta_j|(-1)^j j^4}{4b^+}(2n^2+2n+1) . \tag{41a}$$

The quartic correction to $\Delta\lambda_n$ is thus of zeroth order in $|\theta_1|$ (i.e., independent of it) and roughly proportional to n^2. The corresponding first-order perturbative correction to the $w_{n,\mu}(\xi)$ can be easily shown to be

$$w_{n,\mu}(\xi) = w_{n,\mu}(\xi)_{\text{harm}} + \sum_{n'} \sum_{j=1}^{j_{\max}} [\theta_j(-1)^j j^4/3(b^+)^{1/2}(n'-n)] \int_{-\kappa_{n_{\max}}}^{\kappa_{n_{\max}}} d(\delta\xi) w_{n',\mu}(\delta\xi)_{\text{harm}} \delta\xi^4 w_{n,\mu}(\delta\xi)_{\text{harm}} . \tag{41b}$$

Here the elementary integrals can be evaluated for each n, upon use of $\kappa_{n_{\max}}$ [cf. Eq. (38)], which corresponds to the maximum n value satisfying Eq. (39). Corrections due to $\delta\xi^6$, $\delta\xi^8$, $\delta\xi^{10}$, etc. (which are proportional to $|\theta_1|^{-1/2}$, $|\theta_1|^{-1}$, $|\theta_1|^{-3/2}$, etc., respectively) can be obtained similarly.

The preceding results can be used to study the growth of bandwidth and tunneling depth with n for positive particles. The phase integral over the classically forbidden region $\beta_2^{(n)}$ [Eq. (32b)] can be shown to depend on n [satisfying Eq. (39)] as follows:

$$\beta_2^{(n)} \simeq \left[\int_0^{\pi} d\xi(-q^+(\pi/2)+q^+(\xi))^{1/2}\right] \left\{1-(2n+1)\left[\left[\int_0^{\pi} d\xi(-q^+(\pi/2)+q^+(\xi))^{1/2}\right]^{-1} + (b^{\pm})^{1/2}/q^+(\pi/2)\right] + O(|\theta_1|^{-1})\right\} . \tag{42}$$

Since $q^+(\pi/2)>0$, the n-dependent term in Eq. (42) decreases $\beta_2^{(n)}$ as n grows, thereby increasing the bandwidth according to Eq. (34) and the tunneling depth according to Eq. (32a). The rate of this increase is seen from Eq. (42) to be proportional to $n/|\theta_1|^{1/2}$—a physically plausible result.

For high-lying bands, a detailed calculation of the allowed λ_n can be carried out, in principle, by the following method: Expand $\Delta\lambda$ as a power series in $|\theta_1|$ with unspecified coefficients and terms of the order of $|\theta_1|^{1/2}$, $|\theta_1|^0$, $|\theta_1|^{-1/2}$, $|\theta_1|^{-1}$, ..., $|\theta_1|^{-r+1/2}$; introduce the corrected form $[f^{(r)}(\xi)]^{1/2}$ (cf. Sec. V A), which is accurate to $|\theta_1|^{-r+1/2}$, into $w_n(\xi)$ [Eqs. (B1)—(B6)]; substitute the resulting expressions into Hill's equation and compute the coefficients of the expansion of $\Delta\lambda$ by equating all terms of the same power in $|\theta_1|$ to zero. This method is manageable only numerically, yet it can provide much more insight regarding the γ dependence of the transverse energies than the "many-beam" calculations now in use.[37-39]

As the eigenvalue spectrum is inaccessible analytically for high bound states, their transverse energy must be specified in order to estimate the bandwidth and tunneling depth from Eqs. (32) and (34). We shall obtain such estimates for the case of positive particles. In this case, the classically forbidden region $\alpha_1^{(\lambda)}+\pi-\alpha_2^{(\lambda)}$ is small enough, so that it is well covered by a second-order expansion in $\xi-\alpha_2^{(\lambda)}$ (without violating the condition for the validity of the WKB method, $\beta_2^{(\lambda)} \gg 1$), since the potential crests are high and narrow (Fig. 3). Then we determine, for a given λ, the two turning points $\alpha_1^{(\lambda)}, \alpha_2^{(\lambda)}$ (the two roots of $f_\lambda^+ = 0$) and use $\alpha_2^{(\lambda)}$ (the larger of the two) to evaluate

$$u_1 \equiv -4 \sum_{j=1}^{j_{\max}} j^2 \theta_j^+ \cos(2j\alpha_2^{(\lambda)}) ,$$
$$u_2 \equiv -4 \sum_{j=1}^{j_{\max}} j \theta_j^+ \sin(2j\alpha_2^{(\lambda)}) . \tag{43}$$

Using these expressions, we find, to second order in $\delta\xi = \xi - \alpha_2^{(\lambda)}$ $(0 \le \delta\xi \le |u_2|/u_1)$,

$$\int_0^{\delta\xi} |f_\lambda(\xi)|^{1/2} d(\delta\xi) \simeq -\frac{(u_2)^2}{8(u_1)^{3/2}} \left[\sin^{-1}\left(1-\frac{2u_1}{|u_2|}\delta\xi\right) - \frac{\pi}{2}\right] + \left(1-\frac{u_1\delta\xi}{|u_2|}\right)^{1/2} \left(\frac{|u_2|^{1/2}}{2}\delta\xi^{3/2} - \frac{|u_2|^{3/2}}{4u_1}\delta\xi^{1/2}\right) . \tag{44}$$

To the same accuracy, the bandwidth exponent [Eq. (34)] is found to be

$$\beta_2^{(\lambda)} \simeq \frac{\pi u_2^2}{8u_1^{3/2}} = \frac{\pi|\theta_1|^{1/2}}{4} \left[\sum_{j=1}^{j_{\max}} \phi_j^+ j \sin(2j\alpha_2^{(\lambda)})\right]^2 \Big/ \left|\sum_{j=1}^{j_{\max}} j^2 \phi_j^+ \cos(2j\alpha_2^{(\lambda)})\right|^{3/2} . \tag{45}$$

Equations (44) and (45) can be used in Eq. (B3) or (32a) to obtain the amplitude of the eigenfunction in the classically forbidden region. Estimates of Eq. (44) show that, for

$$\delta\xi \simeq |u_2|/4u_1 \simeq (\alpha_1^{(\lambda)}+\pi-\alpha_2^{(\lambda)})/4 ,$$

the tunneling is still strong, i.e.,

$$\exp\left[-\int_0^{\delta\xi} |f_\lambda^{1/2}(\delta\xi)|\, d(\delta\xi)\right] \gg \exp(-\beta_2^{(\lambda)}) ,$$

whereas for $\delta\xi \simeq |u_2|/2u_1$ it becomes small. Thus, roughly *half of the barrier width is strongly penetrated from both sides* when the crest is high and narrow. This penetration should enhance the Bloch-wave absorption constant (caused by inelastic scattering) (Refs. 20 and 21) compared to that obtained using the single-well approximation[65] (cf. Sec. VI).

For *bound states* (of both negative and positive particles) situated *close to the barrier,* where $\beta_2^{(n)} \lesssim 1$, the conventional WKB approximation fails, and we must resort to the use of the parabolic-cylinder equation as a "comparison equation."[67] In this approximation we define p and $S(\xi)$ as follows:

$$\beta_1^{(p)} = \pi p, \quad \frac{dS}{d\xi} = f_p^{1/2}(\xi)(2p - S^2)^{1/2} . \tag{46}$$

The explicit dependence of S on ξ can be now obtained from

$$S(2p-S^2)^{1/2}/2 + p\sin^{-1}(S/\sqrt{2p}) + \pi/2 = \int_{\alpha_1(p)}^{\xi} f_p^{1/2}(\xi)\, d\xi , \tag{47}$$

and used to approximate the eigenfunctions by

$$w_p(\xi) \simeq [S'(\xi)]^{-1/2}[A^{(p)}D_{p-1/2}(\sqrt{2}S(\xi)) + B^{(p)}D_{p-1/2}(-\sqrt{2}S(\xi))] , \tag{48}$$

where $D_{p-1,2}$ is a fractional-index parabolic-cylinder function. The explicit evaluation of Eq. (48) is possible for the edge of a band of index $p = n + \frac{1}{2}$. Since $n \gg 1$ for high-lying bands, we find, using the appropriate asymptotic form for Hermite functions,[57]

$$w_{n,\mu=0}(\xi) \simeq A^{(n)}(S'(\xi))^{-1/2} \times \begin{cases} (-1)^k(2k-1)!!\cos[\sqrt{4k+1}S(\xi)], & n=2k \\ (-1)^k(2k-1)!!\sin[\sqrt{4k+3}S(\xi)], & n=2k+1 . \end{cases} \tag{49}$$

The eigenfunctions described by Eq. (49) exhibit an oscillatory character in the classically allowed intervals, where $S(\xi)$ is real. They have the form of standing waves and thus constitute a vestige of Bragg reflections, just like $w_n(\xi)$ in Appendix B. Since the classically forbidden intervals are small for levels close to the barrier, there will be no appreciable decay of the amplitude for $\alpha_2^{(n)} < \xi < \alpha_1^{(n)}$, where the argument $S(\xi)$ is complex. This means that tunneling and bandwidth, which are measured by

$$w_n(\xi = \alpha_1^{(n)} + \pi)/w_n(\xi = \alpha_2^{(n)}) ,$$

will be strong.

C. Effects of multiple minima of the potential

A number of experiments have dealt with channeling in composite crystals [e.g., LiF (Ref. 68)], in cases where $q(\xi)$ possesses several minima per unit cell (π period). Multiple minima arise because each unit cell contains atomic planes of different potential strength and sign. In what follows the principles of planar channeling analysis for such cases are presented.

If the transverse energy is such that there are no turning points or two turning points only (Fig. 4), the regimes discussed in Secs. V A–V B are retrieved [although certain formulas no longer apply, e.g., Eq. (36), and all estimates have to be rederived using Eq. (13)]. The nontrivial change from the single-minimum case takes place for transverse energies for which there is more than one pair of turning points—m potential minima allow, at most, $2m$ turning points per π period.

A generalization of the WKB formalism used in Sec. V B to the case of $2m$ turning points[42] $\alpha_1, \ldots, \alpha_{2m}$ ($\alpha_{2m+1} = \delta_1 + \pi$) involves the replacement of the two normalizing constants and the two phase angles characterizing the single-minimum potential eigenfunctions [η_1, η_2 in Eqs. (B1)–(B5)] by $2m$ quantities of each kind. These are determined by the matching conditions at the turning

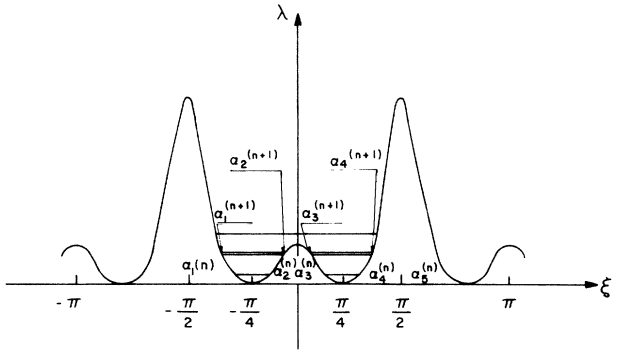

FIG. 4. Potential for positive particles in LiF transverse to (111) planes. The turning points are marked for the bands $n, n+1$. Note that whereas the bands $n, n+2$ are virtually discrete levels, there is a sizable splitting effect on the $(n+1)$th level.

points, by the periodicity, and by the normalization requirements. This WKB approximation is valid when all the phase integrals over the potential crests $\alpha_{2r+2}<\xi<\alpha_{2r+3}$ $(r=0,1,2,\ldots,m-1)$,

$$\beta_{2r+2,2r+3}=\int_{\alpha_{2r+2}}^{\alpha_{2r+3}}|f(\xi)|^{1/2}d\xi \tag{50}$$

are considerably larger than 1.

The quantization condition of the single-minimum case [Eq. (33)] is replaced here by m alternative conditions of the form

$$\beta_{2r+1,2r+2}=\int_{\alpha_{2r+1}}^{\alpha_{2r+2}}d\xi f^{1/2}(\xi)=(n_{2r+1}+\tfrac{1}{2})\pi-\delta_{2r+1}\,,$$
$$\delta_{2r+1}\simeq\exp(-\beta_{2r+2,2r+3})\,, \tag{51}$$

where r is any one value among the $r=0,1,\ldots,m-1$ values labeling the troughs $\alpha_{2r+1}<\xi<\alpha_{2r+2}$. Hence, each single-minimum level is split into m levels which are determined by the different δ_{2r+1} and, in general, the different shapes of $q(\xi)$ in the integrand of each $\beta_{2r+1,2r+2}$. If all $\beta_{2r+2,2r+3}$ are small compared to $\beta_{2m,2m+1}$, the bandwidth of low-lying states due to the overall periodicity, which is governed by $\exp(-\beta_{2m,2m+1})$ will be much smaller than the level splitting governed by $\exp(-\beta_{2r+2,2r+3})$. This can be illustrated for the relatively simple case of two equal minima per π period (Fig. 4), e.g., the (111)-plane potential in LiF.[68] Since $\beta_{4,5}=\beta_{2m,2m+1}$ is very large for $\gamma\gg1$, the effects of overall periodicity for low-lying states become negligible and the problem reduces to that of the ammonia molecule.[69] It is then found that the levels corresponding to odd and even eigenfunctions, which are degenerate in the single-minimum case, are separated by $\sim2\exp(-\beta_{2,3})$.

VI. CONCLUSIONS

In this paper an attempt has been made to improve the analytical treatment of the eigenfunctions and band structure characterizing fast charged particles diffracted in crystals. This attempt has been motivated by the requirements for the analytical study of radiation from the particles, their inelastic scattering, and their interactions with external fields. To comply with these requirements, the following endeavors have been made.

(A) An iterative procedure has been proposed (Sec. II) allowing calculation, to a greater accuracy than in previous attempts,[28–30] of the Fourier components (beam coefficients) of the eigenfunctions that are generated by the longitudinal variation of the potential (LVP) from those BC's that arise due to diffraction in the projected potential. The improved accuracy of this procedure, leading to Eq. (8c), is essential in many cases for a correct evaluation of the intensity of the radiation induced by LVP effects.

(B) A single mathematical apparatus, that of Hill's-equation theory, has been employed to analyze in a systematic, *unified* fashion the variety of diffraction regimes determined by the relativistic mass of the particle and its angle of incidence relative to a set of low-index crystal planes [in the systematic-reflection geometry (SRG)]. This unified treatment of the various regimes is a necessary prerequisite for a unified analysis of radiation from the particle[24] or its inelastic scattering, since such processes can cause transitions between different regimes (by changing both the band index n *and* the potential depth, i.e., the relativistic mass). It also allows one to obtain more analytical information and insight regarding the band structure and the eigenfunctions in the various regimes than the procedures presently in use, by employing several useful calculational methods, among them: (1) Ince's approximations, which can be used to describe the dynamical diffraction of nonrelativistic electrons and positrons in the SRG (Sec. IV B); (2) improved WKB methods which yield nonclassical features (band structure for transversely unbound states—cf. Sec. V A, bandwidth and tunneling for positron channeling states—cf. Sec. V B) that cannot be obtained in the previously used standard WKB approximation[12]; (3) a prescription for the analysis of barrier-region states (Sec. V B); (4) a procedure for the study of channeling in a projected potential with multiple minima per unit cell (Sec. V C).

These methods can be used to investigate radiative and inelastic-scattering effects that have not been revealed by the less refined previously used methods:

(a) The gaps between unbound bands of positrons and electrons of energy below 1 GeV, predicted by Eqs. (31), introduce a rich structure into the spectrum of radiative transitions between unbound states, which is not accounted for by the prevailing models.[31–33]

(b) The penetration of Bloch waves of channeled positrons halfway through the potential barriers about atomic sites, revealed by Eqs. (44) and (45), should augment the absorption (decay) constant of these waves,[21,22]

$$k_n^I\simeq-\int_0^{\pi}d\xi\,U^I(\xi)\,|w_n(\xi)|^2/2k_{0z}\,,$$

because the imaginary reduced potential $U^I(\xi)$ has a part that is strongly localized in the vicinity of atomic sites.[21]

(c) The lack of definite parity by channeling Bloch waves described by Eq. (40) (unless the particle is incident at a Bragg angle), which manifests the periodicity of the projected potential, implies that dipolar transitions with $n_i-n_f=2$ are non-negligible in certain cases, whereas single-channel eigenfunctions[65] forbid such transitions.

(d) Equations (42) and (45) allow investigation of the contribution of the bandwidth of positron channeling states to the linewidth of the radiation they emit. This contribution has been previously obtained only numerically.[37–39]

ACKNOWLEDGMENTS

I am greatly indebted to Dr. J. K. McIver for his valuable assistance and advice to me throughout the work on this paper. I also thank Professor C. Chandler and Professor E. Coutsias for useful discussions. Professor M. O. Scully's continuous encouragement and support are gratefully acknowledged. This work was supported by the U.S. Office of Naval Research.

APPENDIX A: EIGENFUNCTIONS IN THE SHALLOW POTENTIAL

All formulas will be given for centrosymmetric sets of reflections. First we present the "normalized" even and odd solutions, respectively, in the kinematic limit:[49]

$$y_e(\xi)=\cos(\sqrt{\lambda}\xi)-\frac{\sin(\sqrt{\lambda}\xi)}{2\sqrt{\lambda}}\left[|\theta_1|\sum_{j=1}^{j_{\max}}\frac{\phi_j^{\pm}}{j}\sin(2j\xi)\right]$$
$$+\frac{\cos(\sqrt{\lambda}\xi)}{4\lambda}\left[2|\theta_1|\sum_{j=1}^{j_{\max}}\phi_j^{\pm}(1-\cos(2j\xi))-\frac{\theta_1^2}{2}\left[\sum_{j=1}^{j_{\max}}\frac{\phi_j^{\pm}}{j}\sin(2j\xi)\right]^2\right]+O(\lambda^{-3/2}), \tag{A1}$$

$$y_o(\xi)=\frac{\sin(\sqrt{\lambda}\xi)}{\sqrt{\lambda}}+\frac{\cos(\sqrt{\lambda}\xi)}{2\lambda}\left[|\theta_1|\sum_{j=1}^{j_{\max}}\frac{\phi_j^{\pm}}{j}\sin(2j\xi)\right]$$
$$-\frac{\sin(\sqrt{\lambda}\xi)}{4\lambda^{3/2}}\left[2|\theta_1|\sum_{j=1}^{j_{\max}}\phi_j^{\pm}(1+\cos(2j\xi))+\frac{\theta_1^2}{2}\left[\sum_{j=1}^{j_{\max}}\frac{\phi_j^{\pm}}{j}\sin(2j\xi)\right]^2\right]+O(\lambda^{-5/2}). \tag{A2}$$

Second, we write the Ince approximation solutions[53,54] [cf. Eq. (23)] to second order in $|\theta_1|$:

$$y_{n=0}(\mu,\xi)=e^{i\mu\xi}\left[1+\sum_{j=1}^{j_{\max}}\theta_j^{\pm}\left[\frac{1}{2(j^2-\mu^2)}\cos(2j\xi)\frac{-i\mu}{2j(j^2-\mu^2)}\sin(2j\xi)\right]\right.$$
$$\left.+\sum_{j=1}^{j_{\max}}\theta_j^2\left[\frac{(2j^2+\mu^2)\cos(4j\xi)}{16j^2(j^2-\mu^2)(4j^2-\mu^2)}-\frac{3i\mu\sin(4j\xi)}{16j(j^2-\mu^2)(4j^2-\mu^2)}\right]\right], \tag{A3}$$

$$y_{n\neq0}(\mu,\xi)=e^{i\mu\xi}\left[\sin(n\xi-\sigma_n)+\sum_{j=1}^{j_{\max}}\theta_j^{\pm}\sin[(2j+n)\xi-\sigma_n]\right.$$
$$\left.-\sum_{j=n+1}^{j_{\max}}\theta_j^{\pm}\left[\frac{1}{4j(j+n)}\sin[(2j+n)\xi-\sigma_n]-\frac{1}{4j(j-n)}\sin[(2j-n)\xi+\sigma_n]\right]\right]. \tag{A4}$$

APPENDIX B: BOUND SINGLE-MINIMUM EIGENFUNCTIONS IN THE DEEP POTENTIAL

The bound single-minimum potential eigenfunctions are given in the WKB approximation,[62] for $0\le\xi<\alpha_1^{(n)}$, by

$$w_n(\xi)\simeq\frac{A^{(n)}}{|\tilde{f}_n(\xi)|^{1/4}}\left[\sin\eta_1\exp\left[\int_{\xi}^{\alpha_1^{(n)}}d\xi'\,|\tilde{f}_n(\xi')|^{1/2}\right]+\tfrac{1}{2}\cos\eta_1\exp\left[-\int_{\xi}^{\alpha_1^{(n)}}d\xi'\,|\tilde{f}_n(\xi')|^{1/2}\right]\right] \tag{B1}$$

for $\alpha_1^{(n)}<\xi<\alpha_2^{(n)}$, by

$$w_n(\xi)\simeq\frac{A^{(n)}}{[\tilde{f}_n(\xi)]^{1/4}}\cos\left[\int_{\alpha_1^{(n)}}^{\xi}d\xi'\tilde{f}_n^{1/2}(\xi')-\pi/4\right]=\frac{B^{(n)}}{[\tilde{f}_n(\xi)]^{1/4}}\cos\left[\int_{\alpha_1^{(n)}}^{\xi}d\xi'\tilde{f}_n^{1/2}(\xi')+\beta_1+\eta_2-\pi/4\right] \tag{B2}$$

for $\alpha_2^{(n)}<\xi<\alpha_1^{(n)}+\pi$, by

$$w_n(\xi)\simeq\frac{B^{(n)}}{|\tilde{f}_n(\xi)|^{1/4}}\left[\sin\eta_2\exp\left[\int_{\alpha_2^{(n)}}^{\xi}d\xi'\,|\tilde{f}_n(\xi')|^{1/2}\right]+\tfrac{1}{2}\cos\eta_2\exp\left[-\int_{\alpha_2^{(n)}}^{\xi}d\xi'\,|\tilde{f}_n(\xi')|^{1/2}\right]\right], \tag{B3}$$

and, due to the periodicity,

$$w_n(\xi)=\frac{B^{(n)}}{|\tilde{f}_n(\xi)|^{1/4}}\left[\sin\eta_2\exp\left[\beta_2-\int_{\xi}^{\alpha_1^{(n)}}d\xi\,|\tilde{f}_n(\xi)|^{1/2}\right]+\tfrac{1}{2}\cos\eta_2\exp\left[-\beta_2+\int_{\xi}^{\alpha_1^{(n)}}d\xi\,|\tilde{f}_n(\xi)|^{1/2}\right]\right] \tag{B4}$$

for $0\le\xi<\alpha_1^{(n)}$.

In the domain of validity of the WKB approximation, the constants A, B, η_1, and η_2 can be determined from [cf. Eqs. (32) and (33)]

$$\eta_1=n_1\pi+\epsilon_+,\quad \eta_2=n_2\pi+\epsilon_-,\quad \epsilon_{\pm}=\tfrac{1}{2}\delta_n\pm\tfrac{1}{2}[\delta_n^2-\exp(-2\beta_2^{(n)})]^{1/2}, \tag{B5}$$

where n_1 and n_2 are integers,

$$B^{(n)}=(-1)^n2\epsilon_+A^{(n)}\exp(i\pi\mu+\beta_2^{(n)}), \tag{B6}$$

and the normalization condition.

*Present address: Department of Chemistry, Tel-Aviv University, 69978 Ramat-Aviv, Israel.
[1]H. Bethe, Ann. Phys. (Leipzig) **87**, 55 (1928).
[2]C. H. MacGillavry, Physica **7**, 329 (1940).
[3]*Electron Diffraction*, edited by Z. G. Pinsker (Butterworths, London, 1953).
[4]*Electron Diffraction 1927–1977*, edited by P. J. Dobson, J. B. Pendry, and D. J. Humphreys (The Institute of Physics, London, 1978).
[5]J. M. Cowley, *Diffraction Physics* (North-Holland, Amsterdam, 1981).
[6]P. B. Hirsch, A. Howie, R. B. Nicholson, D. W. Pashley, and M. J. Whelan, *Electron Microscopy of Thin Crystals* (Butterworths, London, 1965).
[7]A. Howie, Philos. Mag. **14**, 223 (1966).
[8]M. V. Berry, B. F. Buxton, and A. M. Ozorio de Almeida, Radiat. Eff. **20**, 1 (1973).
[9]Y. Kagan and Y. V. Kononets, Zh. Eksp. Teor. Fiz. **58**, 226 (1970) [Sov. Phys.—JETP **31**, 124 (1970)].
[10]A. M. Ozorio de Almeida, Acta Crystallogr. Sect. A **31**, 435 (1975).
[11]S. V. Plotnikov, D. E. Popov, E. I. Rozum, O. G. Kostareva, and S. A. Vorobiev, Phys. Status Solidi B **103**, 81 (1981).
[12]M. V. Berry, J. Phys. C **4**, 697 (1971).
[13]K. Kambe, G. Lehmpfuhl, and F. Fujimoto, Z. Naturforsch. **29a**, 1034 (1974).
[14]*Channeling*, edited by D. V. Morgan (Wiley, New York, 1973); D. S. Gemmel, Rev. Mod. Phys. **46**, 129 (1974); J. Lindhard, Mat. Fys. Medd. Dansk. Vidensk. Selsk. **34**, No. 14 (1965).
[15]D. F. Lynch, Acta Crystallogr. Sect. A **27**, 399 (1971).
[16]B. F. Buxton, Proc. R. Soc. London, Ser. A **350**, 335 (1976).
[17]N. P. Kalashnikov and M. N. Strikhanov, Kvant. Elektron. (Moscow) **8**, 2293 (1981) [Sov. J. Quantum Electron. **11**, 1405 (1981)].
[18]J. U. Andersen and E. Bonderup, in *Annual Review of Nuclear and Particle Science*, edited by J. B. Jackson (Annual Reviews, Inc., Palo Alto, CA, 1983), Vol. 33.
[19]V. V. Beloshitsky and F. F. Komarov, Phys. Rep. **93**, 117 (1982).
[20]P. M. Dederichs, in *Solid State Physics*, edited by F. Seitz and D. Turnbull (Academic, New York, 1972), Vol. 27, p. 135.
[21]A. Howie and R. M. Stern, Z. Naturforsch. **27a**, 382 (1972); D. Cherns, A. Howie, and M. H. Jacobs, *ibid.* **28a**, 565 (1973).
[22]Y. H. Ohtsuki, Phys. Status Solidi B **67**, 495 (1975); E. Tamura and Y. H. Ohtsuki, *ibid.* **92**, 167 (1979).
[23]J. U. Andersen, E. Bonderup, E. Laegsgaard, and A. H. Sørensen, Phys. Scr. **28**, 308 (1983).
[24]G. Kurizki and J. K. McIver, Phys. Rev. B **32**, 4358 (1985).
[25]J. C. H. Spence, G. Reese, N. Yamamoto, and G. Kurizki, Philos. Mag. B **48**, L39 (1983).
[26]G. M. Reese, J. C. H. Spence, and N. Yamamoto, Philos. Mag. A **49**, 697 (1984).
[27]G. Kurizki and J. K. McIver, Phys. Lett. **89A**, 43 (1982).
[28]G. Kurizki and J. K. McIver, in *LASERS '82 International Conference Proceedings*, edited by R. C. Powell (STS, McLean, VA 1984); in *Free Electron Generators of Coherent Radiation*, edited by C. A. Brau, S. F. Jacobs, and M. O. Scully (SPIE, Bellingam, Washington, 1984), Vol. 453, p. 402.
[29]G. Kurizki, Ph.D. dissertation, University of New Mexico, 1983 (unpublished).
[30]G. Kurizki and J. K. McIver, Nucl. Instrum. Methods B **2**, 67 (1984).
[31]J. U. Andersen, K. R. Eriksen, and E. Laegsgaard, Phys. Scr. **24**, 588 (1981).
[32]A. W. Saenz and H. Uberall, Phys. Rev. B **25**, 4418 (1982).
[33]A. I. Akhiezer, Fiz. Elem. Chastits. At. Yadra **10**, 51 (1979) [Sov. J. Part. Nucl. **10**, 19 (1979)].
[34]Yu. N. Adishchev, A. N. Didenko, V. N. Zabaev, B. N. Kalinin, A. A. Kurkov, A. V. Potylitsin, V. K. Tomchakov, and A. S. Vorobiev, Radiat. Eff. **60**, 61 (1982).
[35]A. V. Andreev, S. A. Akhmanov, V. A. Vysloukh, and V. L. Kuznetsov, Zh. Eksp. Teor. Fiz. **84**, 1743 (1983) [Sov. Phys.—JETP **57**, 1017 (1983)].
[36]D. M. Bird and B. F. Buxton, Proc. R. Soc. London, Ser. A **379**, 459 (1982).
[37]S. Datz, R. W. Fearick, H. Park, R. H. Pantell, R. L. Swent, J. O. Kephart, and B. L. Berman, Nucl. Instrum. Methods B **2**, 74 (1984).
[38]R. L. Swent, R. H. Pantell, M. J. Alguard, B. L. Berman, S. D. Bloom, and S. Datz, Phys. Rev. Lett. **43**, 1723 (1979).
[39]A. V. Tulupov, Radiat. Eff. **62**, 77 (1982).
[40]K. Fujiwara, J. Phys. Soc. Jpn. **17**, 2226 (1961).
[41]V. Weisskopf, Z. Phys. **93**, 561 (1935).
[42]J. Gjønnes, Acta Crystallogr. **15**, 703 (1962).
[43]F. Fujimoto, J. Phys. Soc. Jpn. **14**, 1558 (1959).
[44]B. K. Vainshtein, *Modern Crystallography* (Springer, Berlin, 1981), Vol. 1.
[45]R. V. Vedrinskii and V. S. Malyshevskii, Zh. Eksp. Teor. Fiz. **83**, 899 (1982) [Sov. Phys.—JETP **56**, 506 (1982)].
[46]W. Magnus and S. Winkler, *Hill's Equation* (Interscience, New York, 1966).
[47]P. A. Doyle and P. S. Turner, Acta Crystallogr. Sect. A **24**, 390 (1968). For corrections to the potential due to bonding effects, see, for example, D. J. Smart and D. J. Humphreys, in *Electron Diffraction 1927–1977*, Ref. 4, p. 145.
[48]H. Hochstadt, Arch. Math. **14**, 34 (1963).
[49]H. Hochstadt, Comments Pure Appl. Math. **18**, 353 (1965).
[50]H. Hochstadt, Proc. Am. Math. Soc. **14**, 930 (1963).
[51]H. Hochstadt, Trans. N.Y. Acad. Sci. **26**, 887 (1964).
[52]D. M. Levy and J. B. Keller, Comments Pure Appl. Math. **16**, 469 (1963).
[53]E. L. Ince, Mon. Not. R. Astr. Soc. **75**, 436 (1915).
[54]E. L. Ince, Mon. Not. R. Astr. Soc. **76**, 431 (1916).
[55]R. B. Dingle, Appl. Sci. Res. B **5**, 345 (1956).
[56]J. Heading, *An Introduction to Phase-Integral Methods* (Methuen, London, 1962).
[57]I. S. Gradshteyn and I. M. Ryzhik, *Table of Integrals, Series and Products* (Academic, New York, 1980).
[58]The Fourier expansion of the unbound eigenfunctions can also be derived by means of an improved version of the stationary-phase approximation (cf. Chap. 2 of Refs. 29 and 59).
[59]A. Erdelyi, *Asymptotic Expansions* (Dover, New York, 1956).
[60]A. Erdelyi, Arch. Elek. **29**, 473 (1935).
[61]F. W. J. Olver, *Asymptotics and Special Functions* (Academic, New York, 1974).
[62]M. J. O. Strutt, Math. Z. **49**, 593 (1944).
[63]The proof for the case of Mathieu's equation is found, e.g., in N. W. McLachlan, *Theory and Application of Mathieu Functions* (Dover, New York, 1964). The extension of this proof to Hill's equation is based on the application of Sturm's comparison theorems to the power-series expansion of $q(\xi)$ to show that λ is bounded from above as well as from below by harmonic-oscillator eigenvalues.
[64]More accurate forms of the $w_n(\xi)$ and their beam coefficients for low-lying bands of positive particles can be obtained (cf. Chap. 2 of Ref. 29) using the stationary-phase approximation

in Ref. 59.
[65]M. A. Kumakhov and R. Wedell, Phys. Status Solidi B **84**, 581 (1977).
[66]G. Kurizki (unpublished).
[67]S. C. Miller and R. H. Good, Phys. Rev. **91**, 174 (1953).
[68]B. L. Berman, S. Datz, R. W. Fearick, J. O. Kephart, R. H. Pantell, H. Park, and R. L. Swent, Phys. Rev. Lett. **49**, 474 (1982).
[69]D. M. Dennison and G. E. Uhlenbeck, Phys. Rev. **41**, 313 (1932).